Fabrication of polymer Fabry-Perot fiber sensors using optical fiber microheaters

Mildred S. Cano-Velázquez and Juan Hernández-Cordero*
Instituto de Investigaciones en Materiales, Universidad Nacional Autónoma de México
A.P. 70-360, Cd. Universitaria, México D. F. 04510, México.

ABSTRACT

We report on a novel fabrication technique for polymer based Fabry-Perot (F-P) optical fiber sensors. The F-P interferometers are based on microbubbles generated in the polymer by means of a microheater fiber probe. Upon inserting the probe and a cleaved single-mode fiber in a capillary tube containing the polymer, a microbubble can be readily generated which can serve as a reflective surface. A F-P cavity is thus formed by the microbubble and the single-mode fiber tip and temperature or strain deforming the bubble can be detected upon monitoring the FP resonances. The fabrication and performance of these devices as a temperature sensor is presented in this paper.

Keywords: Optical fiber sensors, Fabry-Perot interferometers, polymer processing, temperature sensors.

1. INTRODUCTION

Interferometric fiber optic sensors have been used extensively in a wide variety of applications, and Fabry-Perot (F-P) sensors in particular represent one of the most versatile configurations[1]. Chemical and physical parameters such as strain, gas concentration, refractive index and temperature have been successfully quantified or monitored using F-P sensors as a key component for compact and high-resolution devices[1, 2]. In general, the materials used within the cavity define the sensitivity and measuring range of these sensors, and the advent of new materials is constantly opening new possibilities for developing compact and highly sensitive devices.

F-P cavities are commonly constructed using to optical fibers in close proximity, thus yielding the so-called Extrinsic Fabry-Perot Interferometric (EFPI) sensor[3, 4]. Typically, these are formed upon placing two optical fibers on opposite ends of a capillary tube with a gap between them. In this approach, fiber positioning within the capillary is critical, since the cavity length effectively defines the spectral response of the sensor. Alternatively, a F-P cavity may be formed upon processing the fiber tip with laser pulses[2], or upon splicing fibers with different geometries such as single-mode and photonic crystal fibers[5]. Recently, EFPI sensors based on microbubbles have been reported; these may be formed during fusion splicing of fibers[6], or via capillary effects in silica tubes spliced to standard single-mode fibers[7]. Strain, pressure and temperature have been measured with these devices over ranges limited by the materials used for fabrication.

We have recently introduced a novel approach for generating microbubbles in liquid media utilizing photothermal effect in carbon nanostructures[8]. Since nanostructures can be readily incorporated onto the endfaces of standard optical fibers, localized heat can be generated using a low power laser diode launched into the fiber core. This arrangement effectively operates as an optical fiber microheater, which among other interesting applications, may be used for generating micron-size bubbles in different liquid media. Taking advantage of the size of these devices, we have successfully used them for fabricating F-P sensors in polymer media[9]. In this paper, we present the latest advances in the manufacturing process of these polymer-based microbubble fiber sensors. The experimental arrangement used for sensor fabrication is based on a computer-controlled system for fiber manipulation and bubble growth monitoring. Capillary tubes filled with polydimethylsiloxane (PDMS) are used for housing both, the sensing fiber and the optical fiber microheater; thus, a microbubble can be generated in the polymer serving as a reflective surface for the F-P cavity. Using motorized actuators, the relative position of the optical fibers and the microheater can be adjusted precisely and the size and location of the bubble can be readily modified. Using signal post-processing, we evaluate features such as sensitivity and the influence of the size of the bubble in the spectral response of the sensors. We further assess the performance of the F-P devices as temperature sensors.

8th Iberoamerican Optics Meeting and 11th Latin American Meeting on Optics, Lasers, and Applications,
edited by Manuel Filipe P. C. Martins Costa, Proc. of SPIE Vol. 8785, 8785C8

2. SENSOR FABRICATION

2.1 Optical fiber microheaters

The F-P sensors are fabricated using optical fiber microheaters developed in our laboratory and these rely on the photothermal effects generated in carbon nanoparticles when irradiated with laser light. A microheater is fabricated via optically driven deposition of carbon nanoparticles onto optical fiber end faces[8]. This is achieved by means of a laser diode (975nm, 200mW max. output power), standard single-mode optical fiber (SMF-28) for laser guiding and deposition, and nanoparticles dissolved in an ethanol solution. The fibers are cleaved and subsequently immersed in the solution; when the laser diode is turned on, the deposition process begins yielding a fiber endface with a layer of nanoparticles.

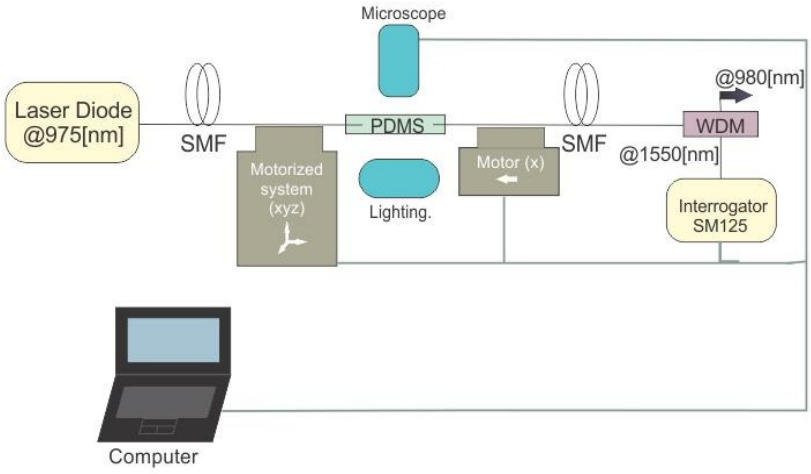

Figure 1. Experimental arrangement for fabrication of F-P sensors: the relative position of the microheater and the sensing fiber is controlled via motorized stages. The process is continuously monitored with a microscope and recorded in a personal computer.

Photothermal effects in nanoparticle clusters arise from enhanced field effects. These have been verified under different experimental conditions when the nanoparticles are irradiated with laser light[10]. In optical fibers with nanoparticle deposits, the localized phothermal effects lead to bubble formation in the vicinity of the fiber tip when immersed in liquid media. Bubbles can thus be generated and their size can be controlled upon adjustments of the output power of the laser diode. The fiber tips effectively operate as microheaters useful for generating micron-size bubbles in liquids with a wide range of viscosities. For the proposed sensors, we focused on polydimethylsiloxane (PDMS), a biocompatible and versatile polymer used in a wide range of applications.

2.2 F-P cavity fabrication

The arrangement for fabrication of the F-P sensors is shown schematically in Figure 1. Glass capillary tubes filled with PDMS are used for hosting both, the fiber microheater and the sensing fiber; these are fed on opposite ends of the capillary tube. Alignment between both fibers is achieved by means of a computer controlled 3D translational stage and the gap between the microheater and the sensing fiber is also adjusted with an additional motorized stage. During the fabrication process, the backreflected signal from the sensing fiber is continuously monitored using a fiber Bragg grating interrogator (Micron Optics, sm125). As seen in the figure, a WDM is used at the input of the interrogator to prevent any residual light from the LD to reach the detection system. Bubble growth and alignment is also monitored during fabrication with a microscope (DinoLite); data and image acquisition together with fiber alignment is conveniently controlled with a virtual instrument developed in LabView.

Initially, a small gap is left between the microheater and the sensing fiber. Once this is fixed, the laser diode is turned on and a bubble starts growing nearby the microheater. When the bubble reaches a target size, the laser diode is turned off; upon adjusting the 3D stage, the fiber microheater is displaced inside the capillary and the bubble can be positioned

within a desired distance from the sensing fiber. The F-P cavity is thus formed between the sensing fiber endface and the microbubble. Finally, if required, the microheater can be carefully removed from the capillary. Figure 2 shows images of two sensors with different spacing between the microbubble and the sensing fiber.

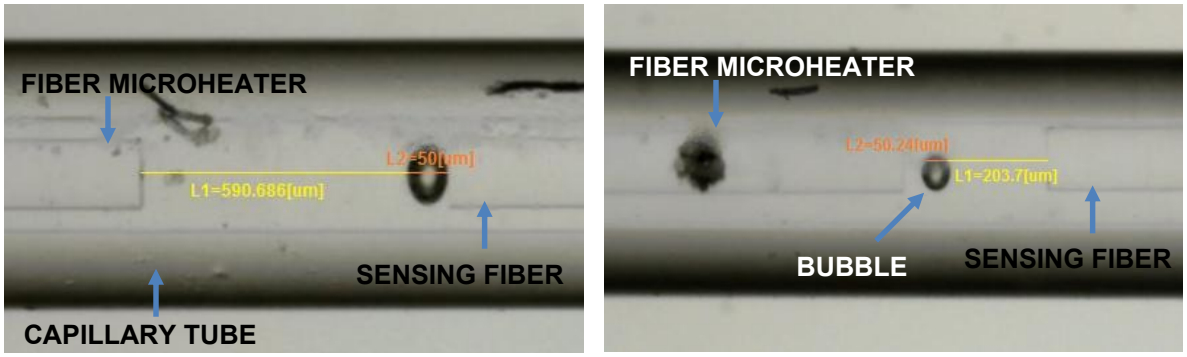

Figure 2. Images of two F-P microbubble polymer sensors with different gaps and bubble sizes. In both cases the fiber microheater remains within the capillary tubes.

3. SPECTRAL FEATURES OF THE F-P SENSORS

As with any F-P cavity, the spectral features of the sensors are given by the geometry and refractive index of the material within the reflective surfaces. In the fiber-bubble configurations, the spectral response depends on the distance between the bubble and the fiber endface (i.e., the gap between the bubble and the fiber tip), the bubble size and the refractive index of the PDMS. The backreflected signal registered by the FBG interrogator is similar to that obtained with multi-mirror F-P interferometers, showing a typical interference signal (carrier), with a short wavelength period, and modulated by an envelope with a longer period.

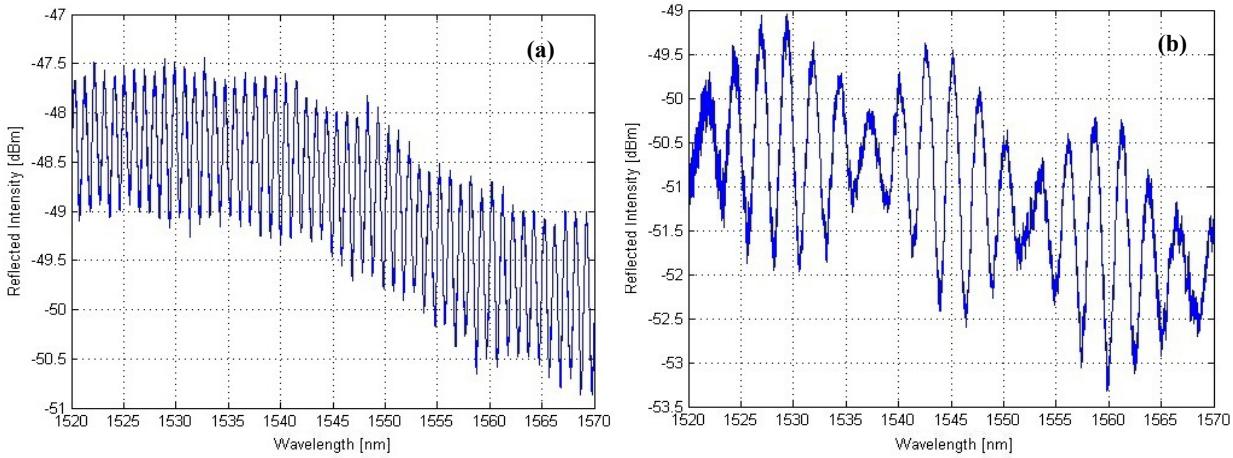

Figure 3. Spectral response of the two sensors shown in Figure 2: (a) large bubble in close proximity to the sensing fiber; (b) small bubble away from the sensing fiber.

Figure 3 shows the interference signals registered with the F-P sensors shown in Figure 2. While a large bubble close to the sensing fiber yields a pattern with practically no modulation envelope (Fig. 3a), a small bubble away from the fiber tip shows a strongly modulated signal (Fig. 3b). Since our setup allows for varying the bubble size and the gap between the bubble and the fiber, we were able to evaluate the effects of these parameters on the spectral response. For a small and fixed gap, an increase in the bubble size yielded only small changes in the modulation index of the envelope. In contrast, for a fixed bubble size, changes in the gap strongly affect the period of the envelope signal. Although further work is required to fully analyze these effects, it is clear that proper signal processing should allow for discerning

between changes in the size of the microbubble and changes in the gap. This should be of interest for sensing applications since temperature and/or strain may affect the bubble and the gap in different ways and this might provide an alternative for a self-referencing scheme.

4. SIGNAL PROCESSING AND ANALYSIS

Signal analysis has been performed following two approaches: one is based on a multi-mirror F-P resonator model and the other through FFT analysis. The theoretical model for data analysis is based on multilayer thin films matrix methods[11]. The incident and transmitted waves are given by:

$$\begin{pmatrix} E_i^+ \\ E_i^- \end{pmatrix} = \frac{1}{t_1 t_2 \dots t_{N-1}} \begin{bmatrix} A & B \\ C & D \end{bmatrix} \begin{pmatrix} E_N^+ \\ E_N^- \end{pmatrix} \quad (1)$$

E_i^+ is the amplitude of the electric field vector on the left-hand side of the input mirror i ($i=1,2,\dots,N$) for a wave front propagating to the right; E_i^- is the amplitude on the left-hand side of mirror i for a wave front traveling to the left; $t_1, t_2, \dots, t_{N-1}$ are transmission amplitude coefficients for every interface, A, B, C and D are the resulting elements of the matrix analysis for the phase changes of the optical wave after multiple reflections inside the cavity.

The transmission amplitude coefficient of the stack of N mirrors is expressed as:

$$t = \frac{t_1 t_2 \dots t_{N-1}}{A - r_N B} \quad (2)$$

where r_N is the reflection amplitude coefficient for the N^{th} interface. The transmission intensity coefficient is given by

$$T = tt^* \quad (3)$$

In our case, the interference pattern observed in the optical interrogator corresponds to the reflection spectrum. Neglecting losses due to absorption, scattering, diffraction or misalignment, the reflection intensity coefficient can be obtained as $R = 1 - T$.

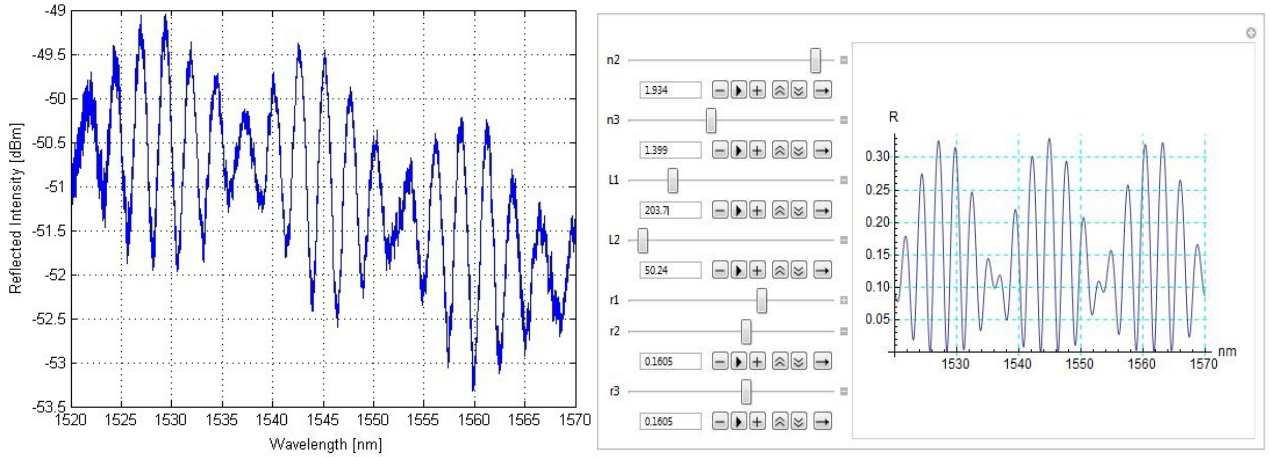

Figure 4. Spectrum registered with the FBG interrogator (left) and its corresponding fitting using the multi-mirror F-P model (right).

The multi-mirror model considers only flat reflective surfaces and allows for adjusting parameters such as the gap between the bubble and the fiber, bubble size and refractive indices. Upon fixing one of these parameters, the model can be used for fitting the experimental spectrum and the values for the remaining parameters can be readily obtained. As shown in Fig. 4, the multi-mirror model fits the registered spectra reasonably well. Nonetheless, calculations can be time consuming and a more efficient scheme is needed for real-time sensor decoding.

Post-processing the spectra with a FFT provides information of the carrier and the envelope of the modulated signal. Through proper scaling of the FFT, the index of the transformation yields the number of peaks within the full spectral range swept by the FBG interrogator. Other features of the signal that are obtained with this analysis include the number of peaks of the envelope and the period of the modulated signal. Through this analysis we were able to investigate the influence of the bubble size and the gap on the modulated signal. This was done upon adjusting the size of the bubble and its position within the capillary tube by means of the LD power and the 3D stage, respectively. While the bubble size only affects the envelope of the signal, the carrier is modified by the gap between the bubble and the sensing fiber.

The curves shown in Figure 5 illustrate the changes in wavelength spacing and number of peaks in the envelope and the carrier. Increasing the bubble size decreases the wavelength spacing and increases the number of peaks registered for the envelope. Similar effects were observed for the carrier but for changes in the gap between the bubble and the sensing fiber. Notice also that the sensitivity to these parameters (e.g., bubble size and gap) is also different in both cases. While changes in the bubble size mostly affect the wavelength spacing of the envelope, changes in the gap affect the number of peaks of the carrier more notably. More experimental work is needed to fully elucidate these effects; nonetheless, this behavior may indicate that a strongly modulated signal and its corresponding FFT could provide a means for discerning between refractive index changes and bubble expansion induced by temperature and/or strain in the F-P sensors.

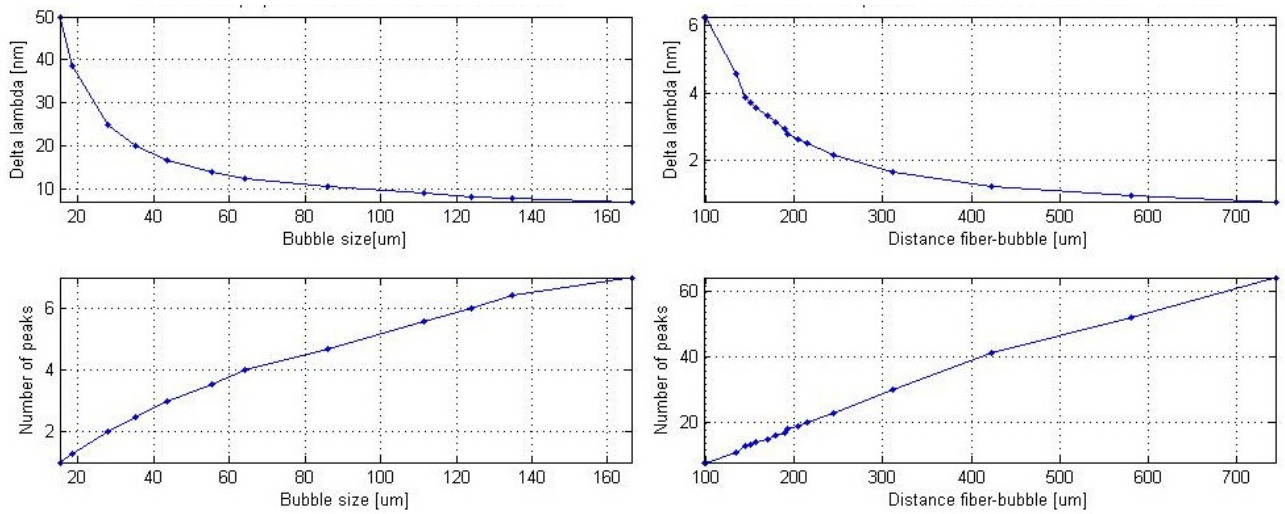

Figure 5. Changes in wavelength spacing and number of peaks of the modulated signal: the bubble size only affects the envelope (left column) and the gap affects the carrier (right column).

5. SENSOR PERFORMANCE: TEMPERATURE RESPONSE

The response of the F-P sensors was evaluated using a glass container with ice and water serving as a thermal bath. A PRT (Platinum Resistive Thermometer) was placed inside the glass in close proximity to the probe to obtain reference values for the changes in temperature. In order to minimize environmental perturbations, the setup was isolated by means of a Plexiglas box. The experimental procedure involved increasing the temperature of a hot plate placed underneath the thermal bath and recording the corresponding spectra registered by the fiber interrogator. With this arrangement, the temperature can be increased up to 70°C and then decreased slowly to room temperature upon turning the hot plate off. Both, the temperature and the corresponding spectrum were recorded periodically over adjustable periods of time and post-processed using both, the multi-mirror F-P model and FFT analysis. Figure 6 shows the spectral shift registered in an F-P sensor for a small range of temperatures.

As shown in Figure 7, post-processing of the experimental data yields the temperature changes as a function of time. The PRT readout is then used as the temperature reference for analyzing the spectral features of the F-P sensors when exposed to temperature changes. As an example, Figure 7 shows the changes in wavelength spacing and the number of

peaks in the spectrum of one sensor as a function of time (i.e., as the temperature is increased). In this case, the spectrum of the F-P probe showed only a small envelope variations (see Fig. 2a) and only the carrier yields useful information. During heating, the wavelength spacing decreases while the number of peaks in the spectrum increase. Following the results shown in Figure 5, the response of this sensor is mostly based on an increase in the gap between the bubble and the sensing fiber (i.e., the length of the F-P cavity), and this can be attributed to thermal expansion and refractive index changes of the PDMS.

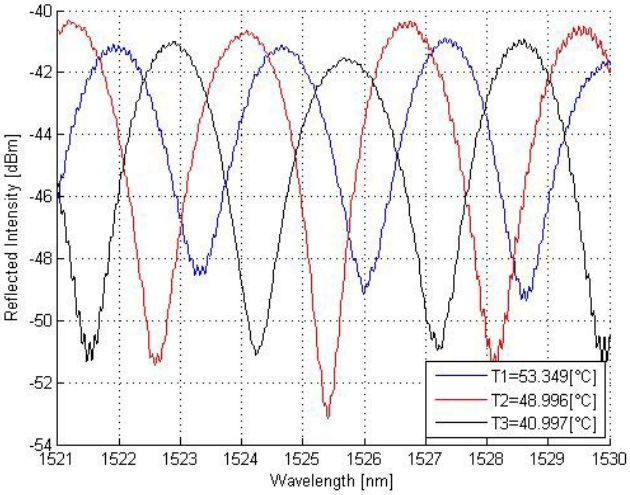

Figure 6. Changes in the backreflected signal regitered with the FBG interrogator for three different temperatures.

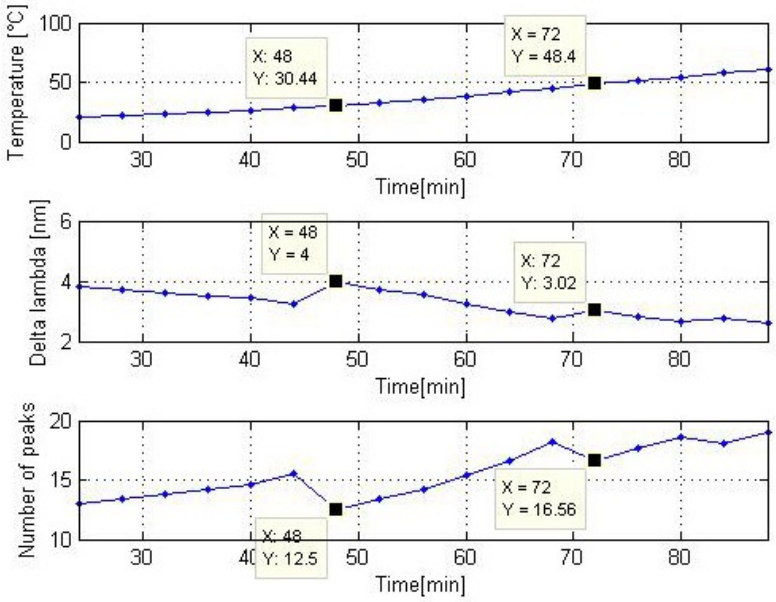

Figure 7. Changes in the spectral features of the F-P sensors registered during heating. The temperature is monitored with a calibrated PRT (a) and spectral features such as wavelength spacing (b) and the number of peaks in the spectrum can be correlated with temperature changes.

Further analysis of the experimental results show that a linear response of the sensors is obtained only for limited ranges of temperature. Notice however that this is due to the periodic response of the F-P cavity and unwrapping algorithms may be used for decoding the sensors over a larger temperature range. As seen in Figure 6, the sensitivity of the sensor varies over different temperature ranges. This is due to the curing process of the PDMS, which requires a thermal

treatment for full solidification. In these experiments, the sensors were left for curing at room temperature for several days; however, thermal curing may yield better results for full polymerizations of the PDMS cavities. We are currently monitoring the curing process of these sensors under temperature cycles as well as for a fixed temperature over extended periods of time. We thus expect to obtain good linearity and consistent sensitivity in the sensor response over extended temperature ranges.

CONCLUSIONS

We have demonstrated a novel method for fabrication of F-P sensors based on optical fiber microheaters. The F-P cavities are formed by the endface of a single-mode optical fiber and a bubble generated by means of the microheater. Using a polymer as a host material (PDMS), the spectral response of the sensors can be adjusted upon varying the size of the bubble and the F-P cavity length. These capabilities could provide a means for adjusting the sensitivity of the sensor to temperature changes or other physical parameters affecting the bubble of the refractive index of the PDMS within the cavity.

Acknowledgments

This work was supported by DGAPA-UNAM through grant PAPIIT-IN102112.

REFERENCES

[1] Lee, B. H., Kim, Y. H., Park, K. S., Eom, J. B., Kim, M. J., Rho, B. S., Choi, H. Y., "Interferometric Fiber Optic Sensors," Sensors, Vol. 12, No. 3, pp. 2467-2486 (2012).

[2] Rao, Y., Deng, M., Duan, M., Yang, X., Zhu, T., Cheng, G., "Micro Fabry-Perot interferometers in silica fibers machined by femtosecond laser," Optics Express, Vol. 15, pp. 14123-14128 (2007).

[3] Jiang, Y., Tang, C., "High-finesse micro-lens fiber-optic extrinsic Fabry–Perot interferometric sensors," Smart Materials and Structures, Vol. 17, No. 5, 055013 (2008).

[4] Wang, G., "High sensitive extrinsic Fabry-Perot interferometric sensor system with low cost," Microwave and Optical Technoly Letters, Vol. 53, No. 7, pp. 1491–1493 (2011).

[5] Milenko, K., Hu, D., Shum, P., Zhang, T., Lim, J., Wang, Y., Wolinski, T., Wei, H., Tong W., "Photonic crystal fiber tip interferometer for refractive index sensing," Optics Letters, Vol. 37, No. 8, pp. 1373-1375 (2012).

[6] Duan, D. , Rao, Y., Hou, Y., Zhu, T., "Microbubble based fiber-optic Fabry-Perot interferometer formed by fusion splicing single-mode fibers for strain measurement," Applied Optics, Vol. 51, No. 8, pp. 1033-1036 (2012).

[7] Wang, Y., Wang, D., Wang, C., Hu, T., "Compressible fiber optic micro-Fabry-Perot cavity with ultra-high pressure sensitivity," Optics Express, Vol. 21, pp. 14084-14089 (2013).

[8] Pimentel-Domínguez, R., Hernández-Cordero, J., Zenit, R., "Microbubble generation using fiber optic tips coated with nanoparticles," Optics Express, Vol. 20, No. 8, pp. 8732-8740 (2012).

[9] Argumedo, B., Márquez, V., Hernández-Cordero, J., "Polymer Microbubble Fabry-Perot Temperature Sensor," in Latin America Optics and Photonics Conference, OSA Technical Digest (online), paper LS3B.5 (2012).

[10] Pimentel-Domínguez, R., Sánchez-Arévalo, F. M., Hautefeuille, M., Hernández-Cordero, J., "Laser induced deformation in polydimethylsiloxane membranes with embedded carbon nanopowder," Smart Materials and Structures, Vol. 22, No. 3, 037001 (2013).

[11] Marquez-Cruz, V., Hernandez-Cordero, J., "Fiber Optic Multimirror Fabry-Perot Sensor for Liquids Analysis," in Latin America Optics and Photonics Conference, OSA Technical Digest (online), paper LS3B.2 (2012).